



THE UNIVERSITY *of* EDINBURGH

Edinburgh Research Explorer

Giant Magnetoresistance in a Molecular Thin Film as an Intrinsic Property

Citation for published version:

Pilia, L, Serri, M, Matsushita, MM, Awaga, K, Heutz, S & Robertson, N 2014, 'Giant Magnetoresistance in a Molecular Thin Film as an Intrinsic Property', *Advanced Functional Materials*, vol. 24, no. 16, pp. 2383-2388. <https://doi.org/10.1002/adfm.201303218>

Digital Object Identifier (DOI):

[10.1002/adfm.201303218](https://doi.org/10.1002/adfm.201303218)

Link:

[Link to publication record in Edinburgh Research Explorer](#)

Document Version:

Peer reviewed version

Published In:

Advanced Functional Materials

Publisher Rights Statement:

Copyright © 2013 WILEY-VCH Verlag GmbH & Co. KGaA, Weinheim. All rights reserved.

General rights

Copyright for the publications made accessible via the Edinburgh Research Explorer is retained by the author(s) and / or other copyright owners and it is a condition of accessing these publications that users recognise and abide by the legal requirements associated with these rights.

Take down policy

The University of Edinburgh has made every reasonable effort to ensure that Edinburgh Research Explorer content complies with UK legislation. If you believe that the public display of this file breaches copyright please contact openaccess@ed.ac.uk providing details, and we will remove access to the work immediately and investigate your claim.



This is the peer-reviewed version of the following article:

Pilia, L., Serri, M., Matsushita, M. M., Awaga, K., Heutz, S., & Robertson, N. (2014). Giant Magnetoresistance in a Molecular Thin Film as an Intrinsic Property. *Advanced Functional Materials*, 24(16), 2383-2388.

which has been published in final form at <http://dx.doi.org/10.1002/adfm.201303218>

This article may be used for non-commercial purposes in accordance with Wiley Terms and Conditions for self-archiving (<http://olabout.wiley.com/WileyCDA/Section/id-817011.html>).

Manuscript received: 17/09/2013; Revised: 04/11/2013; Article published: 16/12/2013

Giant magnetoresistance in a molecular thin film as an intrinsic property**

Luca Pilia,¹ Michele Serri,² Michio M. Matsushita,^{3,*} Kunio Awaga,³ Sandrine Heutz^{2,*} and Neil Robertson^{1,*}

^[1]EaStCHEM, School of Chemistry, Joseph Black Building, University of Edinburgh, West Mains Road, Edinburgh, EH9 3FJ, UK.

^[2]Department of Materials and London Centre for Nanotechnology, Imperial College London, London, UK.

^[3]Department of Chemistry, Graduate School of Science and Research Center of Materials Science, Nagoya University, Chikusa-ku, Nagoya, Japan.

[*]Corresponding authors; neil.robertson@ed.ac.uk, s.heutz@imperial.ac.uk, mmmatsushita@nagoya-u.jp

[**]L.P. thanks the EU Marie Curie programme for funding. The authors thank the EPSRC Global project EP/K004468; the EPSRC project EP/G049726; the Japanese Science and Technology agency; the Leverhulme Trust and the JSPS Core-to-Core programme for supporting the UK-Japan collaboration. M.S. and S.H. thank EPSRC for the grant EP/H002022/1.

Keywords:

spintronics; organic electronics; molecular electronics; magnetic chains; anisotropy

Abstract

We have studied the magnetic, thin-film structural, conductivity and magnetoresistance properties of [Ni(quinoline-8-thiolate)₂] ([Ni(qt)₂]). The conducting and magnetoresistance properties were studied in single crystals and in evaporated thin films through deposition on an interdigitated electrode array. We observe non-linear conductivity interpreted through a space-charge limited conduction mechanism with charges injected from the electrodes. Under applied magnetic field, the material displays giant negative magnetoresistance above 50% at 2 K in both single crystals and in evaporated thin films. The effect can still be observed at 200 K and is interpreted in terms of a double exchange mechanism with the shape of the curve determined by the magnetic anisotropy. The unique observation of GMR as an intrinsic effect in an evaporated thin film of paramagnetic molecules opens up new possibilities in organic spintronics.

1. Introduction

Since the discovery of giant magnetoresistance (GMR) in metallic multilayers in the 1980s, paving the way for modern magnetic data reading^[1] and hybrid logic-storage devices,^[2] the ability to manipulate and detect information using the electronic spin has attracted increasing interest in electronic materials.^[3-7] Spintronics, and related phenomena combining charge transport with magnetic properties, can now be found in inorganic, organic and single-molecule materials and devices showing phenomena including magnetoresistance,^[8] switching,^[9] memory effects^[10] and aimed towards quantum information processing.^[11] Alongside these developments, electronic materials comprising organic or molecular building blocks has exploded into an enormous academic and industrial field including light-emitting devices, photovoltaics and transistors.^[12] The combination of spintronics with organic materials therefore presents a key emerging challenge. The approach of using non-magnetic organic spacers between ferromagnets in a spin-valve structure^[8, 13, 14] is a promising approach but presents challenging interface (or so-called “spinterface”) engineering.^[15, 16, 17] Also, magnetoresistance (MR) has been observed in organic diode structures with non-magnetic electrodes but these still require detailed interpretation.^[18]

An attractive alternative involves use of paramagnetic molecular materials to achieve GMR as this represents a property that is intrinsic to the material itself rather than dependent on the interface, and is well understood through a double-exchange mechanism.^[19] In related fields, multifunctional molecular materials incorporating paramagnetic molecules^[20] have led to a rich series of phenomena, including room-temperature magnetic bistability^[21], non-linear conductivity,^[22] field-induced superconductivity,^[23, 24] conducting ferromagnets^[25] and radical-based conductors.^[26, 27] Regarding GMR in paramagnetic molecular materials however, prior work has been limited to only two families; [TPP][Fe(phthalocyanine)L₂]₂ (L = CN, Cl, Br) and related crystalline salts,^[28-30] and nitronyl nitroxide-tetrathiafulvalene molecules,^{[19, 31-}

^{33]} all studied in the form of brittle single-crystals. The development of molecular materials in practical devices however, requires solution- or vapour-processed polycrystalline or amorphous thin films.^[34] In this context, we report our observation of GMR in vapour-processed films of paramagnetic $[\text{Ni}(\text{qt})_2]$ (**Figure 1**), which opens up new directions in the design of molecular spintronic materials and their application as thin films in devices.

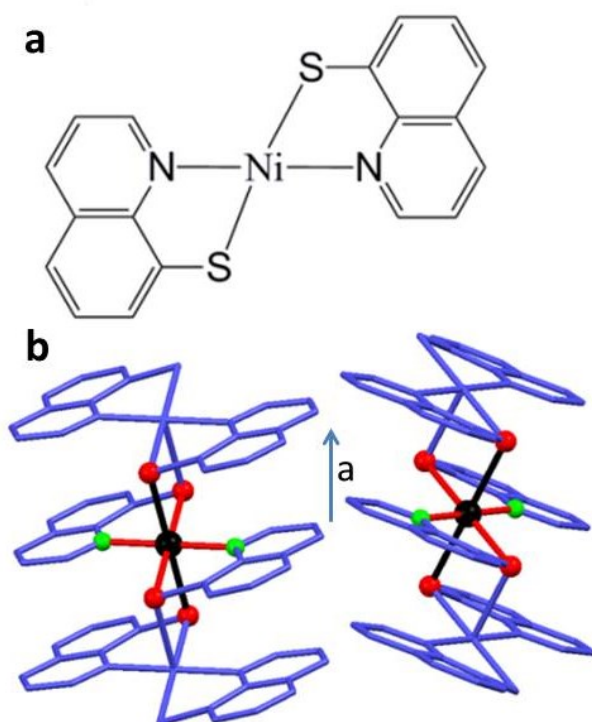


Figure 1. **a** molecular structure of $[\text{Ni}(\text{qt})_2]$. **b** chains along the a -axis formed through axial $\text{Ni}(\text{II})\dots\text{S}$ interactions. The coordination sphere of selected Ni atoms is highlighted (Ni black, S red and N green). The chelate coordination is shown with red bonds and the longer axial interactions with black bonds.

2. Results and Discussion

$[\text{Ni}(\text{qt})_2]$ forms chains where molecules are linked through intermolecular $\text{S}\text{-Ni}$ bonds, with two inequivalent chains oriented along the a -axis (**Figure 1**). Within this structure, $\text{Ni}(\text{II})$ is in a distorted octahedral environment, where the sulfur and nitrogen atoms of the ligands adopt a *trans* geometry within the equatorial plane. Previous studies have highlighted

a weak ferromagnetic interaction and the lack of magnetic saturation at fields up to 70 kOe, attributed to single-ion anisotropy or a spin canted structure.^[35, 36] These magnetic properties, in addition to a strong electron-donating character of $[\text{Ni}(\text{qt})_2]$ in charge transfer salts,^[36] are promising ingredients for MR behaviour and prompted our further study.

2.1. Structural and Magnetic Properties

Firstly, to gain deeper insight into the magnetic anisotropy, we compare crystals aligned perpendicular and parallel to the applied magnetic field. The crystals have a needle-like shape, with the *a*-axis, and therefore the chains, aligned along the long direction (referred to hereafter as the parallel orientation). The χT products for the parallel and perpendicular orientations diverge below 200 K (**Figure 2**) indicating significant anisotropy, with preferential orientation of the magnetic moments in the perpendicular direction. The *g*-factor derived from the high-temperature χT value is 2.53. This is larger than 2.26 reported in the literature,^[36] but the discrepancy can be attributed to the $\sim 10\%$ error in determining the mass of the small single crystal. In keeping with the susceptibility data, the magnetisation (**Figure 2**, **Figure S1**) for parallel crystals increases incrementally with the field, while the perpendicular orientation shows a rapid rise at low temperature although it does not reach saturation at 50 kOe. This again indicates easier magnetisation along the perpendicular direction. The a.c. magnetic susceptibility showed no significant out-of-phase signal down to 2 K, indicating no evidence of spin-glass or single-chain-magnet behaviour, consistent with lack of long range order down to 2 K.^[37]

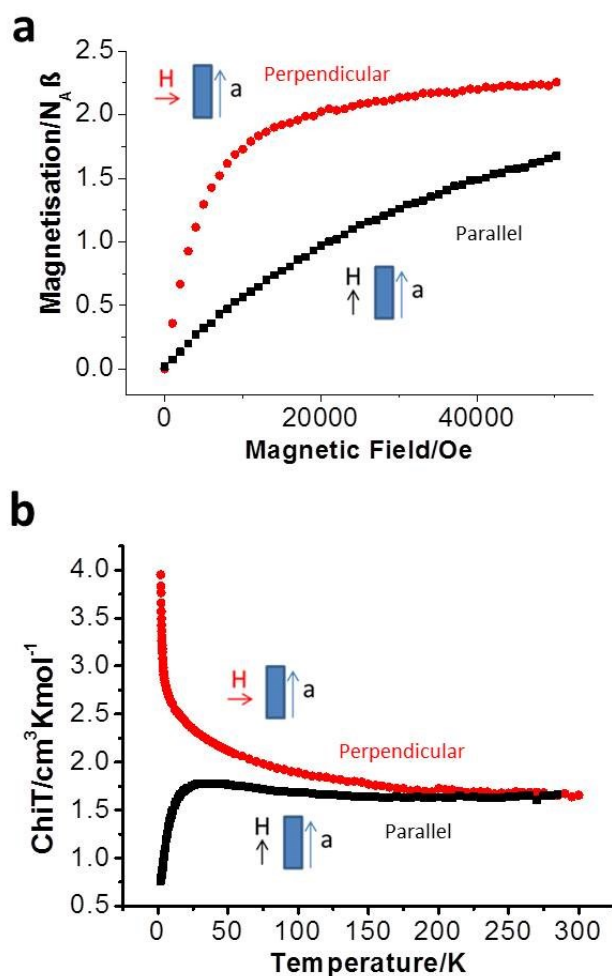


Figure 2. Comparison between magnetisation measurements on crystals aligned perpendicular (red circles) and parallel (black squares) to the applied magnetic field, **a** Magnetisation as a function of field at 2 K. **b** χT product against temperature at field of 1000 Oe.

As discussed above, a key requirement for the implementation of organic-based technology is the ability to process the materials as thin films. We were able to evaporate the material for the first time using organic molecular beam deposition on a range of substrates, including e.g. kapton, silicon and glass. The films display faceted particles with sizes above 100 nm that homogeneously cover the substrate (**Figure 3**) and show a distinctive diffraction pattern (**Figure 4**) on all substrates (**Figure S3**). By randomising the orientation of the particles of a 400 nm thick film, we identified a range of peaks, with the main reflections occurring at 9.8°, 11.6°, and 22.8°, indicating strong preferential orientation within the film

on the substrate. The peak positions differ from those of the bulk material^[35] indicating a different phase, however conversion of the film to the bulk structure upon annealing (**Figures S4, S5**) was observed.

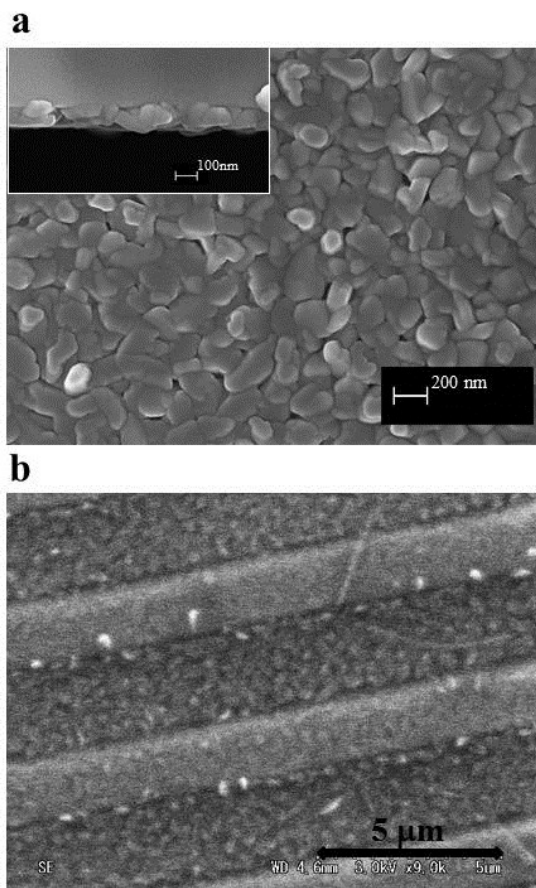


Figure 3. **a**, SEM micrograph of a 75 nm thick film on Si (inset: cross-section). **b**, SEM micrograph of the interdigitated Pt-electrode array with deposited [Ni(qt)₂].

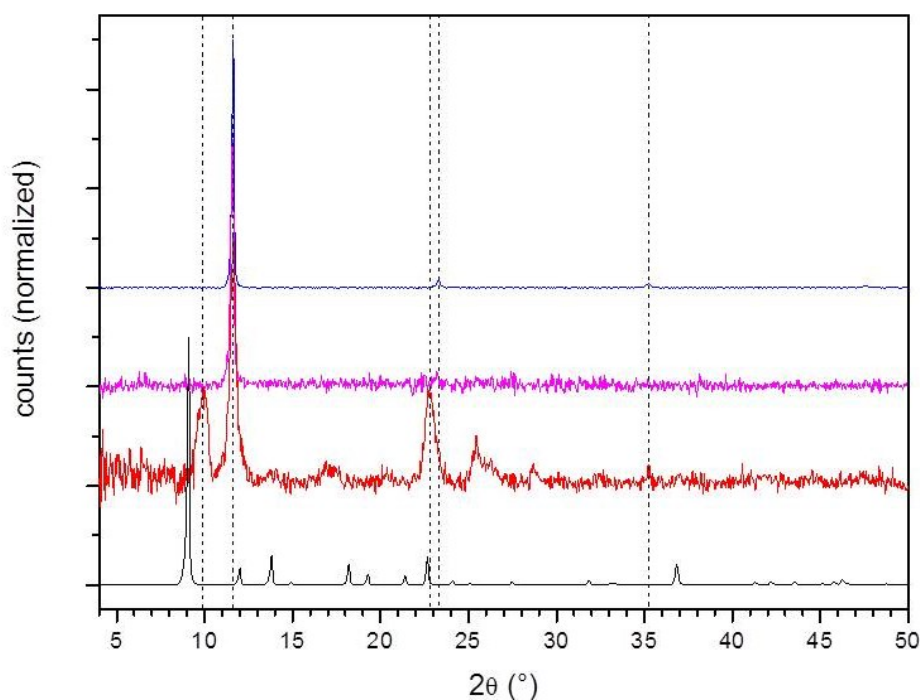


Figure 4. Comparison of out of plane XRD measurements of [Ni(qt)2]: powder before evaporation (black), powder scratched from a 400 nm film (red), thin film (75 nm) on glass (magenta), 400 nm film on glass (blue). The pristine powder XRD pattern corresponds with that calculated from the single crystal X-ray data.^[35]

The magnetic characterisation of a 75 nm film on kapton, reveals an S=1 system (**Figure S2**) which, alongside the ready interconversion through annealing, strongly suggests a similar chain structure to the bulk phase that probably differs only in the chain orientations. At 25 K, the magnetic data are accurately modelled using the Brillouin function, however at lower temperatures the magnetisation is significantly reduced compared to the isotropic spin model (**Figure S2**), and lower than either parallel or perpendicular magnetisation of the crystals. In addition, the curve at 2 K shows a rise at low field that is more rapid than the Brillouin function suggesting the presence of weak ferromagnetism. These factors point to strong anisotropy of the Ni(II) centres that differs in magnitude from that of the powder data.

2.2. Conductivity and Magnetoresistance

Conductivity of the thin film and of $[\text{Ni}(\text{qt})_2]$ single-crystals parallel and perpendicularly-aligned to the current direction were studied on an interdigitated electrode substrate (**Figure 5, Figure S6, Figure S7**). All film and crystal samples showed current vs voltage (I - V) characteristics with strong non-linear behaviour (Figure 5). The currents are very low with low bias voltage, however above a threshold value (≈ 60 V at 2 K) increase exponentially. Similar results were obtained by Komatsu *et al*^[19] in the case of a tetrathiafulvalene-nitronyl nitroxide radical, and the non-linear behaviour explained as a result of a space-charge-limited conduction (SCLC) mechanism^[38, 39] with carriers injected from the electrodes. For $[\text{Ni}(\text{qt})_2]$, the strong electron-donor property^[36] suggests that the injected carriers are holes. Above the threshold voltage, the I - V behaviour can be modelled by an exponential law ($I \propto V^{m+1}$) (Figure 5), with m ranging from 1 to 14 at 200 and 2 K respectively, confirming that the current is dominated by a trapped-charge-limited conduction (TCLC) regime within the SCLC mechanism. In these conditions, the current is due to the bulk properties of the compound rather than the contact effects.

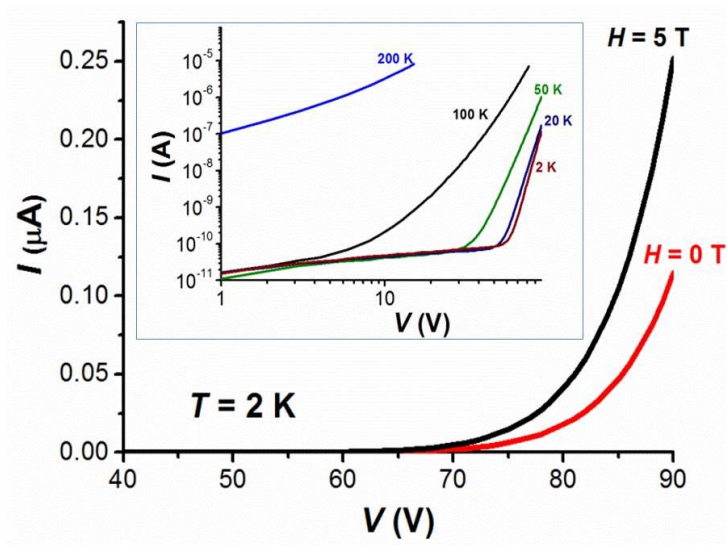


Figure 5. Magnetic field dependence of I - V at 2 K for crystals aligned parallel to the magnetic field; the inset shows the non-linear I - V behaviour for the same device.

The MR effect was measured on the same devices by varying the magnetic field between -5 and 5 Tesla and applying a constant bias voltage, chosen in each case to give a conveniently measureable current within the non-linear region. To avoid the appearance of the Lorentz force the experiment was set up with the magnetic field parallel to the current direction. **Figure 6** shows the magnetic field dependence of resistance of the $[\text{Ni}(\text{qt})_2]$ complex in the oriented crystalline phases and the thin film phase reported as a percentage $(R-R_{0T})/R_{0T}$, where R and R_{0T} are the resistance with and without applied magnetic field, respectively. It is apparent that $[\text{Ni}(\text{qt})_2]$ shows giant negative magnetoresistance in both phases and in both crystal orientations. At 2 K the resistance decreases more than 60% for the crystals and 50% for the thin film, and the effect is still important (10%) at 50 K. Moreover, it is still possible to observe the MR effect up to 200 K, although it has decreased below 1% (**Figure S8**) suggesting that the degree of exchange interaction between the spin of the conduction electrons and those localized at the metal ions is around 200 K. Alternatively, the temperature of the MR may be limited by the magnetisation since the MR is proportional to the square of the magnetisation for the double exchange mechanism (*vide infra*).^[31]

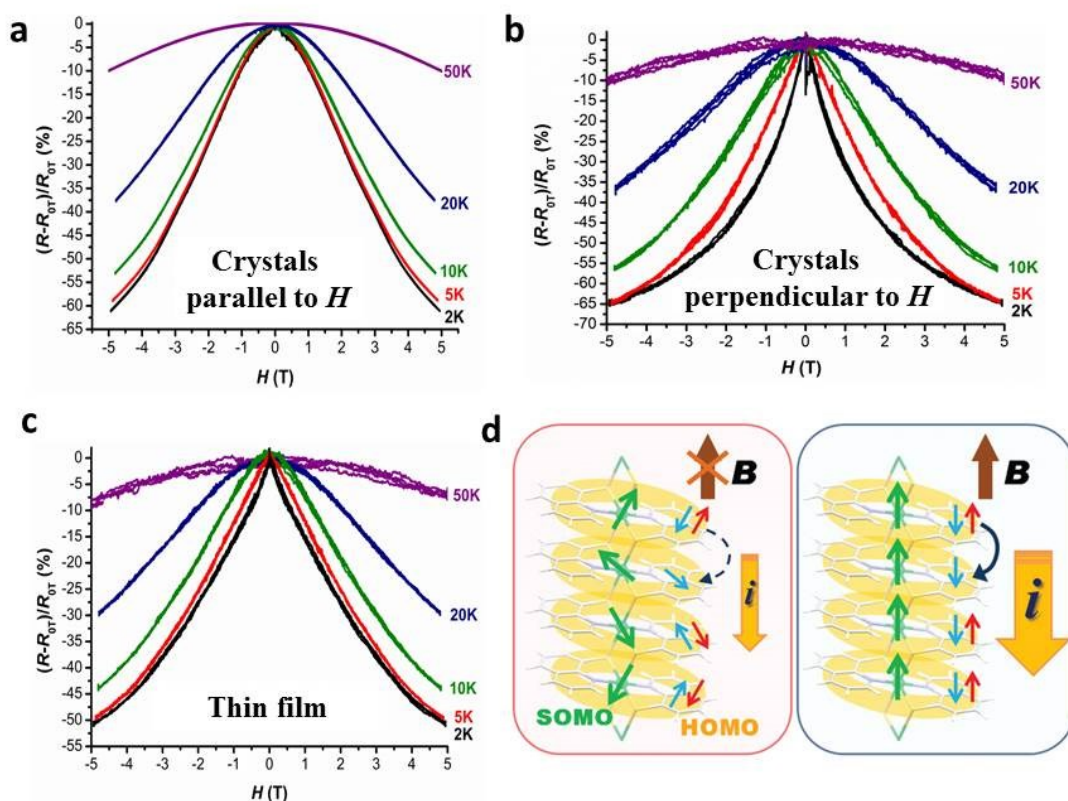


Figure 6. Magnetic field dependence of the magnetoresistance of $[\text{Ni}(\text{qt})_2]$ at various temperatures on **a**, crystals parallel to H and aligned perpendicularly to interdigitated Pt electrodes with $2\ \mu\text{m}$ gap; bias voltage 60V; **b**, crystals perpendicular to H ; bias voltage 85 V; **c**, on thin film deposited onto an identical interdigitated device; bias voltage 75V. **d**, Schematic of the double-exchange mechanism for the GMR. Green arrows show localised unpaired spins of the $S = 1$ centre, red arrows show the α -HOMO electrons and blue arrows show the β -HOMO electrons. The location of the arrows is not representative of the spin density. Calculations indicate the α -electron of the HOMO to be significantly higher in energy than the β -electron hence we show the α -electron to be removed when the hole forms.

2.3. Calculations and Discussion

Calculations at the unrestricted B3LYP/6-31G(d) level of theory were performed on an 8-mer of the chain, with the length chosen to approximate the spin correlation length at low temperature.^[35] These show a fully occupied HOMO possessing predominantly ligand character (**Figure S9**) with SOMO orbitals from the unpaired spins at lower energy, consistent with observations in nitronyl nitroxide-tetrathiafulvalene molecules.^[19] As would

be expected, the spin density is predominantly located around the Ni(II) centre (**Figure S10**).

At high applied electric field, hole doping of the HOMO band occurs, giving rise to a system involving hole transport via the HOMO orbitals based on the quinoxaline ligands, occurring in the presence of the unpaired SOMO spins centred on the Ni(II) centres.

A double exchange mechanism can be used to explain the observed MR as follows. An applied magnetic field will align the localised SOMO spins (Figure 6d) which will couple with the HOMO electrons on the same small-molecule unit. This gives alignment of the spins of the HOMO electrons between neighbouring molecular units, leading to hole hopping with reduced scattering since favourable spin alignment is maintained upon hole transfer. The strong coupling between the HOMO and SOMO spins, due to co-location on a small molecular unit, is consistent with the MR effect persisting to high temperatures.

For the double-exchange mechanism, the MR should scale with the square of the magnetisation.^[31] A comparison was made of MR with magnetisation-squared, both plotted against field for the single-crystal data at 2 K, the conditions under which the curves showed the most distinct shape (**Figure S11**). For both parallel and perpendicular crystal orientations, a clear correlation was shown between the MR and magnetisation-squared, providing strong evidence for the double-exchange mechanism. The crystals show ferromagnetic interactions, however any extended spin correlation does not persist above a few K and MR persists well above 100 K, hence the ferromagnetic exchange is unlikely to be a prerequisite for the MR effect, although it may have an impact on the magnitude and anisotropy of the MR at low temperature (Figure S11).

We note that for the thin-film MR curve, the shape more closely resembles the perpendicular crystal orientation, probably related to the preferred orientation shown within the thin films (Figure S3). Also noteworthy, is that the MR shown in the film phase is of comparable magnitude to that of the single crystals, despite the presence of grain boundaries

in the film. Although the anisotropy of the magnetisation is important in determining the shape of the MR curve, it is apparent that both crystal orientations can display MR to a broadly comparable extent. In fact, the lack of strong dependence on crystal orientation, and the small effect of grain boundaries, are key aspects in MR of the thin-film, which is composed of crystallites where the orientation is likely to be random within the substrate plane (and therefore the current direction), despite the out-of-plane texture.

3. Conclusion

In conclusion, we have observed for the first time giant negative magnetoresistance in a vapour-deposited molecular thin film. The GMR property is intrinsic to the material and not dependent on interface engineering and in this regard falls into the family of small-paramagnetic-molecule GMR materials previously observed using either nitronyl-nitroxide-tetrathiafullerenes or Fe-phthalocyanines. Notably however, $[\text{Ni}(\text{qt})_2]$ is only the second example in the field where no doping and hence no counterion was required, and thus since the material is not a salt, vapour deposition into a thin film was able to be achieved. This ability to deposit $[\text{Ni}(\text{qt})_2]$ as a thin-film demonstrates for the first time that the GMR effect can be observed as an intrinsic property in the type of evaporated polycrystalline film widely applied in the field of organic electronics. The opportunity to build on this finding and develop new materials with related properties opens a new chapter in the joint development of the spintronics and the organic electronics fields towards practical devices.

4. Experimental Section

Materials synthesis and film growth: All chemicals were purchased from Sigma Aldrich and used without further purification. $[\text{Ni}(\text{qt})_2]$ was prepared as previously reported [35]. Anal. calcd for $\text{C}_{18}\text{H}_{12}\text{N}_2\text{NiS}_2$: C 57.02, H 3.19, N 7.39; found: C 56.90, H 3.08, N 7.28. Deposition of $[\text{Ni}(\text{qt})_2]$ thin films for XRD and magnetic characterization was carried out using a SPECTROS OMBD system by Kurt J. Lesker at a growth rate of 0.2 \AA/s , at a pressure of

5×10^{-5} Pa (base pressure 10^{-7} mbar). Devices and films used for the annealing study were prepared via physical vapour deposition (PVD) with sources held in a temperature range between 461 °C and 488 °C at a pressure of $6.8 \cdot 10^{-4}$ Pa. This resulted in a growth rate of 0.1-0.2 Å s⁻¹ which was monitored using a quartz crystal microbalance (QCM). The materials to be sublimed were heated inside an inert crucible by applying a current. Films of 100 nm thickness were produced according to the QCM. The actual film thickness was measured using a profilometer and using the optical absorption of the dissolved film calibrated using solutions of known concentration.

Characterisation: Thin film XRD was carried out on a Rigaku ultraX-18HB at room temperature. Data were collected from 2θ angle of 5–50° at a rate of 3° per minute. Images of the crystal structures were produced using Mercury 2.3[40]. Magnetic susceptibility measurements were performed using a Quantum Design MPMS-XL SQUID magnetometer with MPMS MultiVu Application software to process the data. The temperature dependence of transport properties including magnetoresistance were carried out by utilizing the cryostat of the SQUID magnetometer equipped with a handmade transport probe. Keithley 2487 picoammeter was used for both voltage application and current detection. The measurements were carried out in the dark and under vacuum using a Keithley 2636A sourcemeter equipped with Labtracer 2.0 software. All the conductivity and magnetoresistance measurements were performed on platinum interdigitated electrodes as source and drain, deposited onto a quartz surface with a width of 2 μm and a gap of 2 μm. For the experiments with the crystalline phase the devices were prepared mounting crystals of 1-2 mm length and several μm of width, onto Pt electrodes. Imaging of thin films was carried out using a Hitachi S-4300 Scanning Electron Microscope.

Computational: Calculations were performed with Gaussian 09 Rev.C01, using the unrestricted B3LYP functional and 6-31G(d) basis set with spin multiplicity of the octomer

set for 17 to model the ferromagnetic segment and using the crystal structure geometry [35] without further optimisation. Mercury and Winmostar V3.8 (TENCUBE Institute, Ltd) were used for preparing the molecular coordination and Gaussian input file. MolStudio R4.0 Rev 2.0 program (NEC Corporation) was used for generating MOs and Spin Density images.

Supporting Information

Supporting Information is available online from the Wiley Online Library or from the author.

- _[1] M. N. Baibich, J. M. Broto, A. Fert, F. Nguyen Van Dau, F. Petroff, P. Eitenne, G. Creuzet, A. Friederich, J. Chazelas, *Phys. Rev. Lett.* **1988**, *61*, 2472
- _[2] D. D. Awschalom, M. E. Flatté, *Nature Phys.* **2007**, *3*, 153
- _[3] S. Sanvito, *Chem. Soc. Rev.*, **2011**, *40*, 3336
- _[4] T. D. Nguyen, E. Ehrenfreund, Z. V. Vardeny, *Science*, **2012**, *337*, 204
- _[5] S. D. Jiang, K. Goss, C. Cervetti, L. Bogani, *Science China*, **2012**, *55*, 867
- _[6] P. P. Freitas, F. A. Cardoso, V. C. Martins, S. A. M. Martins, J. Loureiro, J. Amaral, R. C. Chaves, S. Cardoso, L. P. Fonseca, A. M. Sebastião, M. Pannetier-Lecoeur, C. Fermon, *Lab Chip* **2012**, *12*, 546
- _[7] G. Li, S. Sun, R. J. Wilson, R. L. White, N. Pourmand, S. X. Wang, *Sens. Actuators A Phys.* **2006**, *126*, 98
- _[8] Z. H. Xiong, D. Wu, Z. V. Vardeny, J. Shi, *Nature* **2004**, *427*, 821
- _[9] A. Rotaru, I. A. Guralskiy, Gabor, Molnar, L. Salmon, P. Dermont, A. Bousseksou, *Chem. Commun.*, **2012**, *48*, 4163
- [10] J. Lee, E. Lee, S. Kim, G. Sook Bang, D. A. Shultz, R. D. Schmidt, M. D. E. Forbes, H. Lee, *Angew. Chemie Int. Ed.*, **2011**, *50*, 4414
- [11] L. Bogani, W. Wernsdorfer, *Nat. Mater.*, **2008**, *7*, 179
- [12] A. C. Arias, J. D. MacKenzie, I. McCulloch, J. Rivnay, A. Salleo, *Chem. Rev.*, **2010**, *110*, 3

- [13] J-W. Yoo, H. W. Jang, V. N. Prigodin, C. Kao, C. B. Eom, A. J. Epstein, *Phys. Rev. B* **2009**, *80*, 205207
- [14] J-W. Yoo, C-Y. Chen, H. W. Jang, C. W. Bark, V. N. Prigodin, C. B. Eom, A. J. Epstein, *Nat. Mater.*, **2010**, *9*, 638
- [15] P. Ruden, *Nat. Mater.* **2001**, *10*, 8
- [16] D. Sun, L. Yin, C. Sun, H. Guo, Z. Gai, X-G. Zhang, T. Z. Ward, Z. Cheng, J. Shen, *Phys. Rev. Lett.*, **2010**, *104*, 236602
- [17] L. Schulz, L. Nuccio, M. Willis, P. Desai, P. Shakya, T. Kreouzis, V. K. Malik, C. Bernhard, F. L. Pratt, N. A. Morley, A. Suter, G. J. Nieuwenhuys, T. Prokscha, E. Morenzoni, W. P. Gillin, A. J. Drew, *Nature Mater.*, **2011**, *10*, 39
- [18] T. L. Francis, Ö. Mermer, G. Veeraraghavan, M. Wohlgenannt, *New J. Phys.*, **2004**, *6*, 185
- [19] H. Komatsu, M. M. Matsushita, S. Yamamura, Y. Sugawara, K. Suzuki, T. Sugawara, *J. Am. Chem. Soc.* **2010**, *132*, 4528
- [20] I. Ratera, J. Veciana, *Chem. Soc. Rev.*, **2012**, *41*, 303
- [21] W. Fujita, K. Awaga, *Science*, **1999**, *286*, 261
- [22] K. Okamota, T. Tanaka, W. Fujita, K. Awaga, T. Inabe, *Phys. Rev. B.*, **2007**, *76*, 075328
- [23] S. Uji, H. Shinagawa, T. Terashima, T. Yakabe, Y. Terai, M. Tokumoto, A. Kobayashi, H. Tanaka and H. Kobayashi, *Nature*, **2001**, *410*, 908
- [24] H. Fujiwara, H. Kobayashi, E. Fujiwara and A. Kobayashi, *J. Am. Chem. Soc.*, **2002**, *124*, 6816
- [25] E. Coronado, J. R. Galan-Mascaros, C. J. Gomez-Garcia and V. Laukhin, *Nature*, **2000**, *408*, 447
- [26] A. Sarkar, M. E. Itkis, F. S. Tham, R. C. Haddon, *Chem. Eur. J.* **2011**, *17*, 11576

- [27] S. M. Winter, A. R. Balo, R. J. Roberts, K. Lakin, A. Assoud, P. A. Dube, R. T. Oakley, *Chem. Commun.*, **2013**, 49, 1603
- [28] N. Hanasaki, M. Matsuda, H. Tajima, E. Ohmichi, T. Osada, T. Naito, T. Inabe, *J. Phys. Soc. Jpn.*, **2006**, 75, 033703
- [29] D. Ethelbhart, C. Yu, M. Matsuda, H. Tajima, T. Naito, T. Inabe, *Dalton Trans*, **2011**, 40, 2283
- [30] D. Ethelbhart, C. Yu, M. Matsuda, H. Tajima, A. Kikuchi, T. Taketsugu, N. Hanasaki, T. Naito, T. Inabe. *J. Mater. Chem.*, **2009**, 19, 718
- [31] M. M. Matsushita, H. Kawakami, T. Sugawara, M. Ogata, *Phys. Rev. B*, **2008**, 77, 195208
- [32] M. M. Matsushita, H. Kawakami, Y. Kawada, T. Sugawara, *Chem. Lett.* **2007**, 36, 110
- [33] T. Sugawara, H. Komatsu, K. Suzuki, *Chem. Soc. Rev.* **2011**, 40, 3105
- [34] N. Crivillers, M. Mas-Torrent, C. Rovira, J. Veciana, *J. Mater. Chem.*, **2012**, 22, 138833
- [35] T. Miyake, T. Ishida, D. Hashizume, F. Iwasaki, T. Nogami, *Chem. Lett.* **2000**, 952
- [36] T. Miyake, T. Ishida, D. Hashizume, F. Iwasaki, T. Nogami, *Polyhedron* **2001**, 20, 1551
- [37] F-P. Huang, J-L. Tian, D-D. Li, G-J. Chen, W. Gu, S-P. Yan, X. Liu, D-Z. Liao, P. Cheng, *Inorg. Chem.*, **2010**, 49, 2525
- [38] K. C. Kao, W. Hwang, *Electrical Transport in Solids*, Pergamon Press, Oxford, **1981**
- [39] P. E. Burrows, Z. Shen, V. Bulovic, D. M. McCarty, S. R. Forrest, J. A. Cronin, M. E. Thompson, *J. Appl. Phys.* **1996**, 79, 7991
- [40] C. F. Macrae, I. J. Bruno, J. A. Chisholm, P. R. Edgington, P. McCabe, E. Pidcock, L. Rodriguez-Monge, R. Taylor, J. van de Streek, P. A. Wood, *J. Appl. Cryst.* **2008**, 41, 466

